Available online at www.sciencedirect.com

SciVerse ScienceDirect

Ceramics International 38 (2012) 3607–3612

CERAMICS INTERNATIONAL

www.elsevier.com/locate/ceramint

Phase structure and thermophysical properties of co-doped $La_2Zr_2O_7$ ceramics for thermal barrier coatings

Jianying Xiang, Shuhai Chen, Jihua Huang *, Hua Zhang, Xingke Zhao

School of Materials Science and Engineering, University of Science and Technology Beijing, Beijing 100083, China

Received 13 December 2011; received in revised form 28 December 2011; accepted 29 December 2011
Available online 8 January 2012

Abstract

$La_2Zr_2O_7$ has high melting point, low thermal conductivity and relatively high thermal expansion which make it suitable for application as high-temperature thermal barrier coatings. Ceramics including $La_2Zr_2O_7$, $(La_{0.7}Yb_{0.3})_2(Zr_{0.7}Ce_{0.3})_2O_7$ and $(La_{0.2}Yb_{0.8})_2(Zr_{0.7}Ce_{0.3})_2O_7$ were synthesized by solid state reaction. The effects of co-doping on the phase structure and thermophysical properties of $La_2Zr_2O_7$ were investigated. The phase structures of these ceramics were identified by X-ray diffraction, showing that the $La_2Zr_2O_7$ ceramic has a pyrochlore structure while the co-doped ceramics $(La_{0.7}Yb_{0.3})_2(Zr_{0.7}Ce_{0.3})_2O_7$ and the $(La_{0.2}Yb_{0.8})_2(Zr_{0.7}Ce_{0.3})_2O_7$ exhibit a defect fluorite structure, which is mainly determined by ionic radius ratio $r(A_{av.}{}^{3+})/r(B_{av.}{}^{4+})$. The measurements for thermal expansion coefficient and thermal conductivity of these ceramics from ambient temperature to 1200 °C show that the co-doped ceramics $(La_{0.7}Yb_{0.3})_2(Zr_{0.7}Ce_{0.3})_2O_7$ and $(La_{0.2}Yb_{0.8})_2(Zr_{0.7}Ce_{0.3})_2O_7$ have a larger thermal expansion coefficient and a lower thermal conductivity than $La_2Zr_2O_7$, and the $(La_{0.2}Yb_{0.8})_2(Zr_{0.7}Ce_{0.3})_2O_7$ shows the more excellent thermophysical properties than $(La_{0.7}Yb_{0.3})_2(Zr_{0.7}Ce_{0.3})_2O_7$ due to the increase of Yb_2O_3 content.

Keywords: Thermal conductivity; Thermal expansion; Ceramic; Co-doping

1. Introduction

Thermal barrier coatings (TBCs) are widely used in turbine engines to protect hot-section metallic components from corrosion and oxidation [1,2]. The conventional TBCs material in commercial use is stabilized zirconia with 8 wt.% yttria (8YSZ). However, it could hardly be used for long-term application at temperatures above 1200 °C due to its low sintering resistance and low phase structure stability, which increases thermal conductivity and makes them less effective [3,4]. In the next generation of advanced engines, further increase in thrust-to-weight ratio will require even higher gas turbine inlet temperature. So it is urgently needed to develop new TBCs materials with a significantly lower thermal conductivity and better sintering resistance than 8YSZ [5]. However, the selection of TBCs materials is restricted by some basic requirements such as high melting point, low thermal conductivity, high thermal expansion coefficient, high phase stability, and low sintering rate [6,7]. It is found by many researchers [8–10] that the rare earth zirconates show promising thermophysical properties. Its general composition is $A_2B_2O_7$, where A is a 3^+ cation (La to Lu) and B is a 4^+ cation (Zr, Ce, Hf, etc.), such as $La_2Zr_2O_7$, it has excellent thermal stability, low sintering rate and low thermal conductivity. However, its thermal expansion is low compare to 8YSZ ($9.1 \times 10^{-6}\ K^{-1}$ at 1000 °C for $La_2Zr_2O_7$ and $10.1 \times 10^{-6}\ K^{-1}$ at 1000 °C for 8YSZ) [11–13].

In recent studies, it has been reported that materials with lower thermal conductivity and higher thermal expansion coefficient can be prepared by doping or co-doping with one or more oxides (Yb_2O_3, CeO_2, Gd_2O_3, Sm_2O_3, and Nd_2O_3) due to defect cluster formation, which indicates that the thermal conductivity of $La_2Zr_2O_7$ may be reduced further by doping with other elements in the cation of La or Zr [14,15]. Clarke and coworkers [16] also points out that substituted cation, especially the atom with large atomic weight, at site A or B creates mass disorder on the cation sublattice, which results in the lowering of thermal conductivity. Meanwhile the thermal expansion coefficient is proved to be higher by Cao et al. [17].

The primary objective of the present work was to devise approaches to further lower the thermal conductivity and higher

* Corresponding author. Tel.: +86 10 62334859; fax: +86 10 62334859.
E-mail address: jihuahuang47@sina.com (J. Huang).

0272-8842/$36.00
doi:10.1016/j.ceramint.2011.12.077

the thermal expansion coefficient of $La_2Zr_2O_7$. Oxides co-doping approach was used where part of cations A and B were substituted by other elements in $La_2Zr_2O_7$ ceramic. The $La_2Zr_2O_7$, $(La_{0.7}Yb_{0.3})_2(Zr_{0.7}Ce_{0.3})_2O_7$ and $(La_{0.2}Yb_{0.8})_2(Zr_{0.7}Ce_{0.3})_2O_7$ ceramics were synthesized by solid state reaction. Their thermal conductivities and thermal expansion coefficients were measured, and the effects of co-doping on the phase structure and thermophysical properties were also investigated.

2. Experiment

In the present study, ZrO_2 (Shanghai St-Nano Science and Technology Co. Ltd., purity ≥99.99%), La_2O_3, Yb_2O_3 and CeO_2 (GRIPM Advanced Materials Co. Ltd., purity ≥99.99%) were chosen as the reactants. The oxide powders were fired at 900 °C for 5 h before weighing. After mixed the stoichiometric constituents of $La_2Zr_2O_7$, $(La_{0.7}Yb_{0.3})_2(Zr_{0.7}Ce_{0.3})_2O_7$ and $(La_{0.2}Yb_{0.8})_2(Zr_{0.7}Ce_{0.3})_2O_7$ by ball milling in analytically pure alcohol and dried at 110 °C for 6 h in vacuum drying oven, these ceramics were synthesized by solid state reaction at 1600 °C for 12 h.

For thermal conductivity measurements, these ceramics powder were uniaxially hot-pressed into disk-shaped samples with Φ12.7 × (2–3) mm using a 12.7 mm diameter graphite die at 1600 °C and 45 MPa pressure for 4 h. The hot-pressed pellets were heat treated for 6 h at 800 °C in air for oxidation of the surface carbon layer deposited on the samples during hot pressing.

The phase structure of each ceramic was characterized by X-ray diffraction (XRD, Rigaku D/Max 2500, Japan) with Ni filtered Cu Kα radiation (0.1542 nm) at the scanning rate of 4°/min. The microstructure of the pellets was examined using field emission scanning electron microscopy (FESEM, ZEISS ULTRA55). The bulk densities (ρ) of hot-pressed pellets were measured by the Archimedes principle with an immersion medium of deionized water.

The specific heat capacities (C_p) of these ceramics were measured using differential scanning calorimetry (DSC, Netzsch DSC204-F1, Germany) in the range of ambient temperature to 1200 °C. The thermal expansion coefficients of these ceramics were determined with a high-temperature dilatometer (Netzsch DIL402C/7, Germany) from ambient temperature to 1200 °C at a heating rate of 5 °C/min in argon atmosphere. The size of samples is approximately Φ10 × 6 mm. The hot-pressed pellets of three ceramics were used for thermal diffusivity (λ) measurements. Thermal diffusivity testing of the ceramic discs was carried out using laser-flash method on the laser flash apparatus (Netzsch LFA427, Germany) in an argon atmosphere. Before measurements, both the front and back faces of these samples were coated with a thin layer of colloidal graphite. These coatings were done to prevent direct transmission of laser beam through the translucent specimen at high temperatures. Each specimen was measured three times at room temperature, 200 °C, 400 °C, 600 °C, 800 °C, 1000 °C and 1200 °C.

The thermal conductivities (k) of the samples were calculated by the following equation with specific heat capacity (C_p), density (ρ) and thermal diffusivity (λ):

$$\kappa = \lambda \cdot \rho \cdot C_p \quad (1)$$

Because the sintered samples were not fully dense (100%), the measured values of thermal conductivity were modified for the actual value k_0 using the following Eq. (2), where φ is the fractional porosity [18].

$$\frac{k}{k_0} = 1 - \frac{4}{3}\varphi \quad (2)$$

3. Results and discussion

3.1. Microstructure and relative density

The typical microstructure of $(La_{0.7}Yb_{0.3})_2(Zr_{0.7}Ce_{0.3})_2O_7$ and $(La_{0.2}Yb_{0.8})_2(Zr_{0.7}Ce_{0.3})_2O_7$ ceramics is shown in Fig. 1. The interfaces between grains are very clean, the gap is very small and no other interphases and unreacted oxides existed in boundaries between grains. Fig. 2 shows the relative density of $La_2Zr_2O_7$, $(La_{0.7}Yb_{0.3})_2(Zr_{0.7}Ce_{0.3})_2O_7$ and $(La_{0.2}Yb_{0.8})_2(Zr_{0.7}Ce_{0.3})_2O_7$ ceramics sintered at 1600 °C and 45 MPa pressure for 4 h. Each specimen has a high relative density due to the high temperature and high pressure in the hot pressing process.

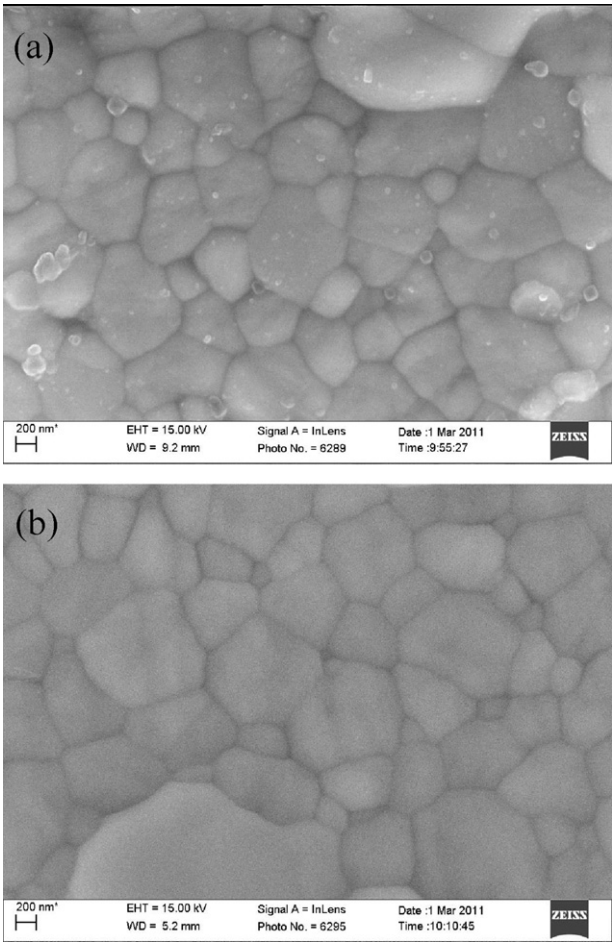

Fig. 1. Typical microstructure of $(La_{0.7}Yb_{0.3})_2(Zr_{0.7}Ce_{0.3})_2O_7$ (a) and $(La_{0.2}Yb_{0.8})_2(Zr_{0.7}Ce_{0.3})_2O_7$ (b) ceramics.

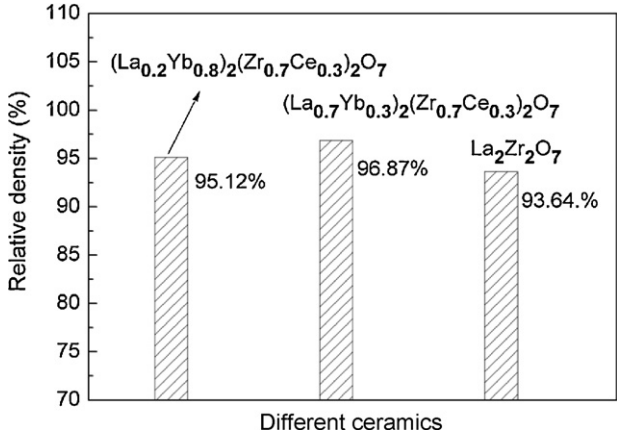

Fig. 2. Relative density of $La_2Zr_2O_7$, $(La_{0.7}Yb_{0.3})_2(Zr_{0.7}Ce_{0.3})_2O_7$ and $(La_{0.2}Yb_{0.8})_2(Zr_{0.7}Ce_{0.3})_2O_7$ ceramics.

3.2. Phase structure

Fig. 3(a) shows the X-ray diffraction patterns of $La_2Zr_2O_7$, $(La_{0.7}Yb_{0.3})_2(Zr_{0.7}Ce_{0.3})_2O_7$ and $(La_{0.2}Yb_{0.8})_2(Zr_{0.7}Ce_{0.3})_2O_7$ ceramics. It can be seen that $La_2Zr_2O_7$ ceramic has a single pyrochlore structure which is characterized by the presence of typical super-lattice peaks at 2θ values of about 14° (1 1 1), 28° (3 1 1), 37° (3 3 1) and 45° (5 1 1) using Cu Kα radiation [19], whereas the $(La_{0.7}Yb_{0.3})_2(Zr_{0.7}Ce_{0.3})_2O_7$ and $(La_{0.2}Yb_{0.8})_2(Zr_{0.7}Ce_{0.3})_2O_7$ ceramics exhibit a defect fluorite structure. X-ray diffraction patterns of these ceramics in the $(1\,1\,1)_F$/$(2\,2\,2)_{Py}$ peak are shown in Fig. 3(b), the peak of $(La_{0.7}Yb_{0.3})_2(Zr_{0.7}Ce_{0.3})_2O_7$ and $(La_{0.2}Yb_{0.8})_2(Zr_{0.7}Ce_{0.3})_2O_7$ shifts to the large 2θ-side, indicating that Yb_2O_3 and CeO_2 were dissolved in $La_2Zr_2O_7$ crystal.

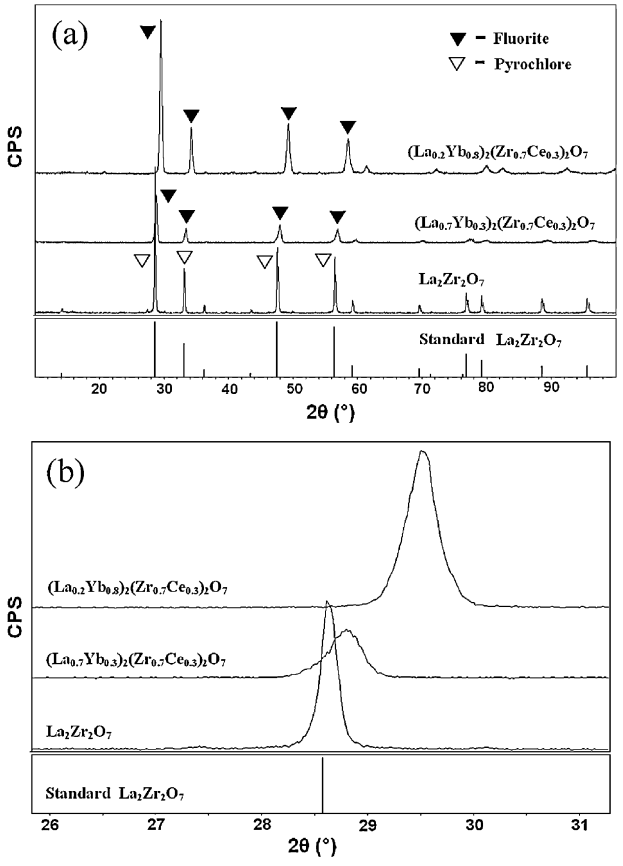

Fig. 3. XRD patterns of $La_2Zr_2O_7$, $(La_{0.7}Yb_{0.3})_2(Zr_{0.7}Ce_{0.3})_2O_7$ and $(La_{0.2}Yb_{0.8})_2(Zr_{0.7}Ce_{0.3})_2O_7$ ceramics: (a) 2θ range of 10–90°; (b) the single $(1\,1\,1)_F$/$(2\,2\,2)_{Py}$ peak in a 2θ range of 28–30°.

In the $A_2B_2O_7$ system, the crystal structure is mainly determined by the ionic radius ratio $r(A^{3+})/r(B^{4+})$ of A and B cations. The stability of pyrochlore structure in zirconates is limited to the range of $1.46 \leq r(A^{3+})/r(B^{4+}) \leq 1.78$, and the fluorite oxide will form if the $r(A^{3+})/r(B^{4+})$ is lower than 1.40 [20]. For the complex rare-earth zirconates, the ionic radius ratio can be estimated from the ionic radius of the component ions and the chemical composition using the following equation [21]:

$$\frac{r(A_{av.}{}^{3+})}{r(B_{av.}{}^{4+})} = \frac{[xr(La^{3+}) + (1-x)r(Yb^{3+})]}{[yr(Zr^{4+}) + (1-y)r(Ce^{4+})]} \quad (3)$$

where x, $(1-x)$, y, $(1-y)$ are the composition of each atom.

The ionic radius of La^{3+} and Yb^{3+} are 1.160 Å and 0.858 Å while the Zr^{4+} and Ce^{4+} are 0.720 Å and 0.970 Å, respectively. The values of $r(A_{av.}{}^{3+})/r(B_{av.}{}^{4+})$ for $La_2Zr_2O_7$, $(La_{0.7}Yb_{0.3})_2(Zr_{0.7}Ce_{0.3})_2O_7$ and $(La_{0.2}Yb_{0.8})_2(Zr_{0.7}Ce_{0.3})_2O_7$ ceramics can be calculated by the Eq. (3) with above mentioned ionic radiuses, and the values are equal to 1.64, 1.345 and 1.155, respectively. Both of co-doped ceramics are smaller than 1.40 due to the co-doping in the La and Zr sites, which reveals that the co-doping in $La_2Zr_2O_7$ can cause the transformation from pyrochlore to defect fluorite structure.

3.3. Thermal conductivity

Fig. 4 shows the specific heat capacity of $La_2Zr_2O_7$, $(La_{0.7}Yb_{0.3})_2(Zr_{0.7}Ce_{0.3})_2O_7$ and $(La_{0.2}Yb_{0.8})_2(Zr_{0.7}Ce_{0.3})_2O_7$ as a function of temperature. From all curves illustrated in Fig. 4, the specific heat capacity increases with the increases of temperature. The co-doped ceramics $(La_{0.7}Yb_{0.3})_2(Zr_{0.7}Ce_{0.3})_2O_7$ and $(La_{0.2}Yb_{0.8})_2(Zr_{0.7}Ce_{0.3})_2O_7$ have a lower specific

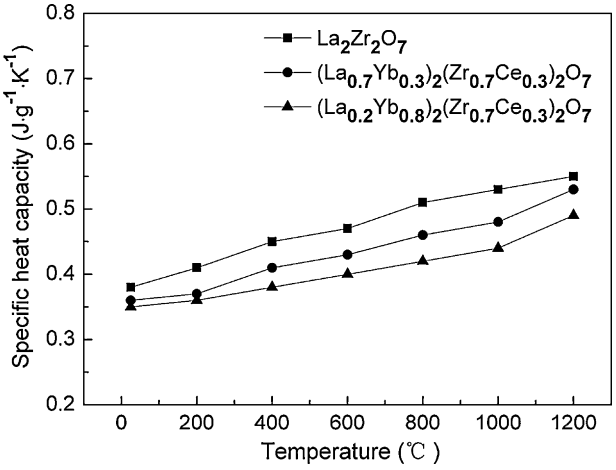

Fig. 4. Specific heat capacity of $La_2Zr_2O_7$, $(La_{0.7}Yb_{0.3})_2(Zr_{0.7}Ce_{0.3})_2O_7$ and $(La_{0.2}Yb_{0.8})_2(Zr_{0.7}Ce_{0.3})_2O_7$ ceramics as a function of temperature.

heat capacity than $La_2Zr_2O_7$, and the $(La_{0.2}Yb_{0.8})_2(Zr_{0.7}Ce_{0.3})_2O_7$ is lower than $(La_{0.2}Yb_{0.8})_2(Zr_{0.7}Ce_{0.3})_2O_7$ under identical temperature conditions due to the increase of Yb_2O_3 content, which is consistent with the Neumann–Kopp rule [1].

The thermal diffusivities of $La_2Zr_2O_7$, $(La_{0.7}Yb_{0.3})_2(Zr_{0.7}Ce_{0.3})_2O_7$ and $(La_{0.2}Yb_{0.8})_2(Zr_{0.7}Ce_{0.3})_2O_7$ at various temperatures are shown in Fig. 5. Clearly, the measured thermal diffusivities of these ceramics monotonically decrease with the increases of temperature from room temperature to 1200 °C, which suggests a dominant phonon conduction behavior in most polycrystalline materials [22]. In this investigation, the thermal diffusivities of $La_2Zr_2O_7$, $(La_{0.7}Yb_{0.3})_2(Zr_{0.7}Ce_{0.3})_2O_7$ and $(La_{0.2}Yb_{0.8})_2(Zr_{0.7}Ce_{0.3})_2O_7$ from room temperature to 1200 °C are located within the range of 0.523–0.905, 0. 464–0.703 and 0.455–0.551 $mm^2\,s^{-1}$, respectively. Both of co-doped $La_2Zr_2O_7$ ceramics have lower thermal diffusivity than $La_2Zr_2O_7$, and the $(La_{0.2}Yb_{0.8})_2(Zr_{0.7}Ce_{0.3})_2O_7$ shows the lowest thermal diffusivity among these ceramics.

The thermal conductivity of $La_2Zr_2O_7$, $(La_{0.7}Yb_{0.3})_2(Zr_{0.7}Ce_{0.3})_2O_7$ and $(La_{0.2}Yb_{0.8})_2(Zr_{0.7}Ce_{0.3})_2O_7$ ceramics as a function of temperature are plotted in Fig. 6 according to Eq. (1) with the specific heat capacity (C_p), density (ρ) and thermal diffusivity (λ). The values in Fig. 6 were corrected to 100% theory density according to Eq. (2). It can be seen that the thermal conductivities of these ceramics decrease gradually as temperature increases almost throughout the present temperature range, and the thermal conductivities of co-doped ceramics $(La_{0.7}Yb_{0.3})_2(Zr_{0.7}Ce_{0.3})_2O_7$ and $(La_{0.2}Yb_{0.8})_2(Zr_{0.7}Ce_{0.3})_2O_7$ are lower than $La_2Zr_2O_7$. According to the micro-mechanism of thermal conduction, the thermal conduction of inorganic non-metallic material is the result of phonon impacting, and the thermal conductivity of phonon is shown by the following equation [23]:

$$k = \frac{1}{3} C_v \cdot \overline{V} \cdot \overline{l} \tag{4}$$

where C_v is the specific heat capacity of the phonon, $\overline{V}$ is the average speed of phonon, and $\overline{l}$ is the mean free path of phonon. C_v is almost a constant when temperature is on Debye temperature. The value of $\overline{V}$ is related with elastic ratio (E) and density (ρ), because of the effect of temperature on the elastic ratio and density is not obvious, so the value of $\overline{V}$ may be also as a constant approximately. Consequently, the value of thermal conductivity (k) is mainly decided by the phonon mean free path which is proportional to the square of the differences of mass and ionic radius between the substituted and the substituting atoms [24,25]. Because the weights of substituted atoms Yb and Ce (173.00 and 140.10, respectively) are higher than the La and Zr (138.91 and 91.22, respectively), and the ionic radius are different between Yb^{3+} and La^{3+} (1.061 Å and 0.858 Å), Ce^{4+} and Zr^{4+} (0.790 Å and 0.920 Å), the effective of phonon scattering by the co-doping cations is significantly stronger. Consequently, the thermal conductivities of $(La_{0.2}Yb_{0.8})_2(Zr_{0.7}Ce_{0.3})_2O_7$ and $(La_{0.7}Yb_{0.3})_2(Zr_{0.7}Ce_{0.3})_2O_7$ are lower than that of $La_2Zr_2O_7$, and the $(La_{0.2}Yb_{0.8})_2(Zr_{0.7}Ce_{0.3})_2O_7$ ceramic has lower thermal conductivity than $(La_{0.7}Yb_{0.3})_2(Zr_{0.7}Ce_{0.3})_2O_7$ due to the increase of Yb_2O_3 content. The thermal conductivities of $(La_{0.2}Yb_{0.8})_2(Zr_{0.7}Ce_{0.3})_2O_7$ and $(La_{0.7}Yb_{0.3})_2(Zr_{0.7}Ce_{0.3})_2O_7$ are located within1.42–1.69 $W\,m^{-1}\,K^{-1}$and 1.32–1.47 $W\,m^{-1}\,K^{-1}$, respectively, which are also clearly lower than current 8YSZ (3.0 at room temperature to 2.12 $W\,m^{-1}\,K^{-1}$ at 1273 K) [1,25,26].

3.4. Thermal expansion coefficient

The thermal expansion coefficient of $La_2Zr_2O_7$, $(La_{0.7}Yb_{0.3})_2(Zr_{0.7}Ce_{0.3})_2O_7$ and $(La_{0.2}Yb_{0.8})_2(Zr_{0.7}Ce_{0.3})_2O_7$ are presented in Fig. 7. The thermal expansion coefficient is proportional to the average distance between particles among the lattice, which is related to the strength of the ionic bonds [27]. The strength of the ionic bond is given in the following equation [28]:

$$I_{A-B} = 1 - e\frac{(x_A - x_B)^2}{4} \tag{5}$$

where I_{A-B} is the strength of the ionic bond between cations at sites A and B, x_A is the average electronegativity of cations at

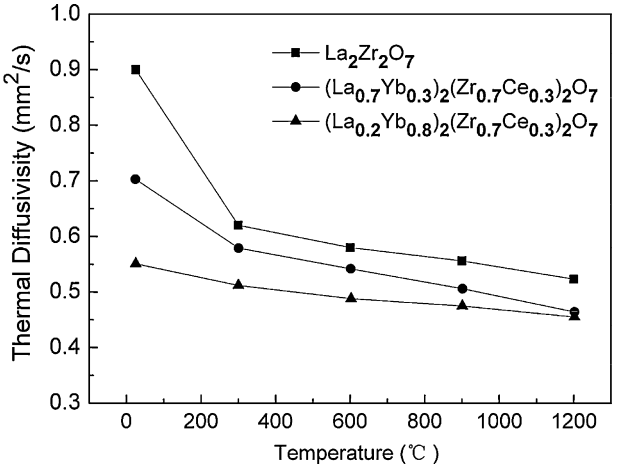

Fig. 5. Thermal diffusivity of $La_2Zr_2O_7$, $(La_{0.7}Yb_{0.3})_2(Zr_{0.7}Ce_{0.3})_2O_7$ and $(La_{0.2}Yb_{0.8})_2(Zr_{0.7}Ce_{0.3})_2O_7$ ceramics as a function of temperature.

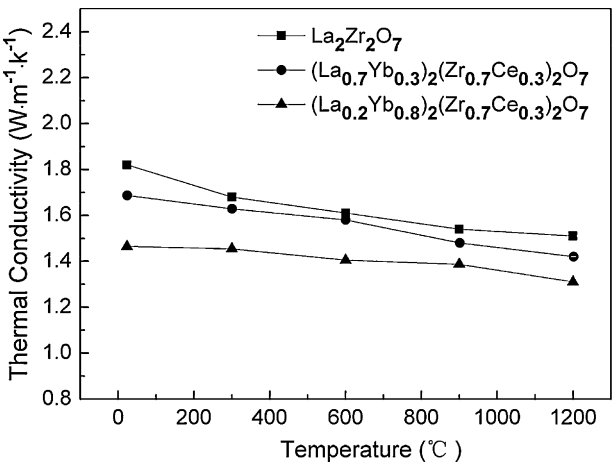

Fig. 6. Thermal conductivity of $La_2Zr_2O_7$, $(La_{0.7}Yb_{0.3})_2(Zr_{0.7}Ce_{0.3})_2O_7$ and $(La_{0.2}Yb_{0.8})_2(Zr_{0.7}Ce_{0.3})_2O_7$ ceramics as a function of temperature.

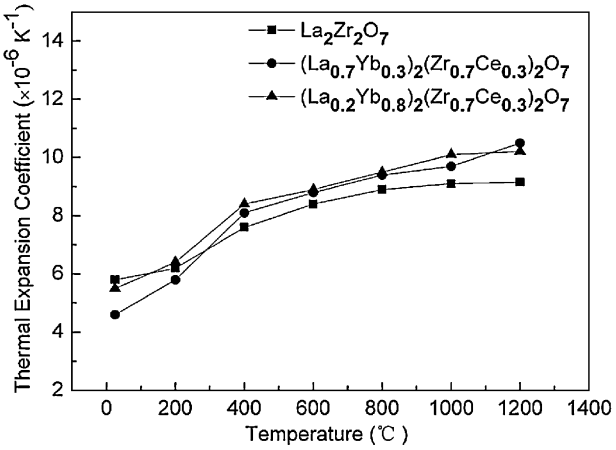

Fig. 7. Thermal expansion coefficient of $La_2Zr_2O_7$, $(La_{0.7}Yb_{0.3})_2(Zr_{0.7}Ce_{0.3})_2O_7$ and $(La_{0.2}Yb_{0.8})_2(Zr_{0.7}Ce_{0.3})_2O_7$ ceramics as a function of temperature.

site A, and x_B is the average electronegativity of cations at site B. Therefore, the thermal expansion coefficients decrease with the electronegativity difference between cations at sites A and B decreasing. It can be seen that the thermal expansion coefficients of the co-doped ceramics increase gradually with the temperature increases up to 1200 °C, the value is $10.5 \times 10^{-6}\,K^{-1}$ for $(La_{0.7}Yb_{0.3})_2(Zr_{0.7}Ce_{0.3})_2O_7$ and $10.21 \times 10^{-6}\,K^{-1}$ for $(La_{0.2}Yb_{0.8})_2(Zr_{0.7}Ce_{0.3})_2O_7$, which are both higher than the $La_2Zr_2O_7$ reported by Vassen and Zhou, and are also higher than that of 8YSZ by Busso et al. [12,13,29]. The improvement in thermal expansion coefficient can be attributed to the relative lower electronegativity of the Yb and Ce cations.

4. Conclusions

The $La_2Zr_2O_7$ and its co-doped ceramics $(La_{0.7}Yb_{0.3})_2(Zr_{0.7}Ce_{0.3})_2O_7$ and $(La_{0.2}Yb_{0.8})_2(Zr_{0.7}Ce_{0.3})_2O_7$ were synthesized by solid state reaction at 1600 °C for 12 h. The $La_2Zr_2O_7$ has a pyrochlore structure while the $(La_{0.7}Yb_{0.3})_2(Zr_{0.7}Ce_{0.3})_2O_7$ and $(La_{0.2}Yb_{0.8})_2(Zr_{0.7}Ce_{0.3})_2O_7$ ceramics exhibit a defect fluorite structure, which is mainly determined by the ionic radius ratio $r(A_{av.}{}^{3+})/r(B_{av.}{}^{4+})$. The co-doped ceramics $(La_{0.7}Yb_{0.3})_2(Zr_{0.7}Ce_{0.3})_2O_7$ and $(La_{0.2}Yb_{0.8})_2(Zr_{0.7}Ce_{0.3})_2O_7$ have larger thermal expansion coefficient than $La_2Zr_2O_7$ due to the relative lower electronegativity of the substituted atoms of Yb and Ce, whereas their thermal conductivities are lower than $La_2Zr_2O_7$, and the $(La_{0.2}Yb_{0.8})_2(Zr_{0.7}Ce_{0.3})_2O_7$ ceramic shows the lowest thermal conductivity because of the increase of Yb_2O_3 content in doped sites, which is located within 1.315–1.465 W m^{-1} K^{-1}. Therefore, the co-doped ceramics $(La_{0.7}Yb_{0.3})_2(Zr_{0.7}Ce_{0.3})_2O_7$ and $(La_{0.2}Yb_{0.8})_2(Zr_{0.7}Ce_{0.3})_2O_7$ are two promising candidates for high-temperature TBCs.

Acknowledgments

This work was financially supported by the National Basic Research Program (973 Program) of China under Grant No. 61311203B. The authors are grateful to Prof. Huibin WU for his assistance in the preparation of hot-pressed samples.

References

[1] Z.G. Liu, J.H. Ouyang, B.H. Wang, Y. Zhou, J. Li, Thermal expansion and thermal conductivity of $Sm_xZr_{1-x}O_{2-x/2}$ ceramics, Ceram. Int. 35 (2009) 791–796.
[2] S.Q. Guo, Y. Kagawa, Effect of thermal exposure on hardness and Young's modulus of EB-PVD yttria-partially-stabilized zirconia thermal barrier coating, Ceram. Int. 33 (3) (2007) 263–270.
[3] H.C. Wang, C.L. Wang, W.B. Su, J. Liu, H. Peng, Y. Sun, Synthesis and thermoelectric performance of Ta doped $Sr_{0.9}La_{0.1}TiO_3$ ceramics, Ceram. Int. 37 (7) (2011) 2609–2613.
[4] W. Ma, H. Dong, H. Guo, S. Gong, X. Zheng, Thermal cycling behavior of $La_2Ce_2O_7$/8YSZ double-ceramic-layer thermal barrier coatings prepared by atmospheric plasma spraying, Surf. Coat. Technol. 204 (21–22) (2010) 3366–3370.
[5] Z. Xu, L. He, H. Zhao, R. Mu, S. He, X. Cao, Composition, structure evolution and cyclic oxidation behavior of $La_2(Zr_{0.7}Ce_{0.3})_2O_7$ EB-PVD TBCs, J. Alloys Compd. 491 (1–2) (2010) 729–736.
[6] X. Cao, R. Vassen, D. Stoever, Ceramic materials for thermal barrier coating, J. Eur. Ceram. Soc. 24 (2004) 1–10.
[7] V.K. Tolpygo, D.R. Clarke, Morphological evolution of thermal barrier coatings induced by cyclic oxidation, Surf. Coat. Technol. 163–164 (2003) 81–86.
[8] Z. Liu, J. Ouyang, Y. Zhou, X. Xia, Structure and thermal conductivity of $Gd_2(Ti_xZr_{1-x})_2O_7$ ceramics, Mater. Lett. 62 (2008) 4455–4457.
[9] L. Liu, Q. Xu, F. Wang, H. Zhang, Thermalphysical properties of complex rare-earth zirconate ceramic for thermal barrier coating, J. Am. Ceram. Soc. 91 (2008) 2398–2401.
[10] H. Zhou, D. Yi, H. Zhong, Dy and Ce co-doped $La_2Zr_2O_7$ ceramic powder used for thermal barrier coating, J. Inorg. Mater. 23 (3) (2008) 567–572.
[11] R. Vassen, X. Cao, F. Tietz, D. Basu, D. Stöver, Zirconates as new materials for thermal barrier coatings, J. Am. Ceram. Soc. 83 (8) (2000) 2023–2028.
[12] X. Cao, R. Vassen, W. Jungen, S. Schwartz, F. Tietz, D. Stöver, Thermal stability of lanthanum zirconate plasma-sprayed coating, J. Am. Ceram. Soc. 84 (9) (2001) 2086–2090.
[13] E.P. Busso, J. Liu, S. Sakurai, M. Nakayama, A mechanistic study of oxidation-induced degradation in a plasma-sprayed thermal barrier system, Acta Mater. 49 (9) (2001) 1515–1528.
[14] D. Zhu, R.A. Miller, Thermal conductivity and sintering resistance of advanced thermal barrier coatings, Ceram. Eng. Sci. Proc. 23 (2002) 457–468.
[15] J.R. Nicholls, K.J. Lawson, A. Johnstone, D.S. Rickerby, Methods to reduce the thermal conductivity of EB-PVD TBCs, Surf. Coat. Technol. 151–152 (2002) 383–391.
[16] M.R. Winter, D.R. Clarke, Oxide materials with low thermal conductivity, J. Am. Ceram. Soc. 90 (2) (2007) 533–540.
[17] X. Cao, R. Vassen, F. Tietz, Lanthanum–cerium oxide as a thermal barrier-coating material for high-temperature applications, Adv. Mater. 5 (17) (2003) 1438–1442.
[18] Q. Xu, W. Pan, J. Wang, C. Wan, L. Qi, H. Miao, Rare-earth zirconate ceramics with fluorite structure for thermal barrier coatings, J. Am. Ceram. Soc. 89 (1) (2006) 340–342.
[19] B.P. Mandal, A.K. Tyagi, Preparation and high temperature-XRD studies on a pyrochlore series with the general composition $Gd_{2-x}Nd_xZr_2O_7$, J. Alloys Compd. 437 (1–2) (2007) 260–263.
[20] M.A. Subramanian, G. Aravamudan, S. Rao, Ferromagnetic $R_2Mn_2O_7$ pyrochlores (R = D, Lu, Y), Prog. Solid State Chem. 72 (1) (1988) 24–30.
[21] H. Yamamura, H. Nishino, K. Kakinuma, K. Nomura, Electrical conductivity anomaly around fluorite–pyrochlore phase boundary, Solid State Ionics 158 (3–4) (2003) 359–365.
[22] G.E. Youngblood, R.W. Rice, R.P. Ingel, Thermal diffusivity of partially and fully stabilized (yttria) zirconia single crystals, J. Am. Ceram. Soc. 71 (4) (1984) 255–260.
[23] H. Zhou, D. Yi, Effect of rare earth doping on thermo-physical properties of lanthanum zirconate ceramic for thermal barrier coating, J. Rare Earths 26 (6) (2008) 770–774.

[24] R. Mévrel, J. Laizet, A. Azzopardi, B. Leclercq, M. Poulain, O. Lavigne, D. Demange, Thermal diffusivity and conductivity of $Zr_{1-x}Y_xO_{2-x/2}$ ($x = 0$, 0.084 and 0.179) single crystals, J. Eur. Ceram. Soc. 24 (2004) 3081–3089.

[25] J. Wu, X. Wei, N.P. Padture, P.G. Klemens, M. Gell, E. García, Low-thermal-conductivity rare-earth zirconates for potential thermal-barrier-coating applications, J. Am. Ceram. Soc. 85 (2002) 3031–3035.

[26] D. Zhu, R. Miller, Thermal conductivity and elastic modulus evolution of thermal barrier coatings under high heat flux conditions, J. Therm. Spray Technol. 9 (2009) 175–180.

[27] J. Wang, L. Li, B.J. Campbell, Z. Lvc, Y. Ji, Y. Xue, Structure, thermal expansion and transport properties of $BaCe_{1-x}Eu_xO_{3-\delta}$ oxides, Mater. Chem. Phys. 86 (2004) 150–155.

[28] H. Zhang, Q. Xu, F. Wang, L. Liu, Y. Wei, X. Chen, Preparation and thermophysical properties of $(Sm_{0.5}La_{0.5})_2Zr_2O_7$ and $(Sm_{0.5}La_{0.5})_2(Zr_{0.8-}Ce_{0.2})_2O_7$ ceramics for thermal barrier coatings, J. Alloys Compd. 475 (2009) 624–628.

[29] H. Zhou, D. Yi, Z. Yu, Preparation and thermophysical properties of CeO_2 doped $La_2Zr_2O_7$ ceramic for thermal barrier coatings, J. Alloys Compd. 438 (2006) 217–221.